Received: 18 December 2021 | Revised: 18 February 2022 | Accepted: 2 March 2022

DOI: 10.1111/ppl.13661

ORIGINAL ARTICLE

Physiologia Plantarum

Desiccation tolerance in bryophytes relates to elasticity but is independent of cell wall thickness and photosynthesis

Alicia V. Perera-Castro[1,2] | Jaume Flexas[1,3]

[1]Department of Biology, Universitat de les Illes Balears, INAGEA, Palma de Mallorca, Spain

[2]Department of Botany, Ecology and Plant Physiology, Universidad de La Laguna, Av. Astrofísico Francisco Sánchez, La Laguna, Spain

[3]King Abdulaziz University, Jeddah, Saudi Arabia

Correspondence
Alicia V. Perera-Castro, Universidad de La Laguna, Av. Astrofísico Francisco Sánchez, La Laguna, Spain.
Email: pereraalicia11@gmail.com

Funding information
Ministerio de Ciencia, Innovación y Universidades (MCIU, Spain) and the ERDF (FEDER), Grant/Award Number: PGC2018-093824-B-C41; Ministerio de Educación, Cultura y Deporte (MECD, Spain), Grant/Award Number: FPU-02054

Edited by K.-J. Dietz

Abstract

Mosses have been found outliers of the trade-off between photosynthesis and bulk elastic modulus described for vascular plants. Hence, potential trade-offs among physical features of cell walls and desiccation tolerance, water relations, and photosynthesis were assessed in bryophytes and other poikilohydric species. Long-term desiccation tolerance was quantified after variable periods of desiccation/rehydration cycles. Water relations were analyzed by pressure–volume curves. Mesophyll conductance was estimated using both CO_2 curve-fitting and anatomical methods. Cell wall elasticity was the parameter that better correlated with the desiccation tolerance index for desiccation tolerant species and was antagonistic to higher absolute values of osmotic potential. Although high values of cell wall effective porosity were estimated compared with the values assumed for vascular plants, the desiccation tolerance index negatively correlated with the porosity in desiccation tolerant bryophytes. Neither cell wall thickness nor photosynthetic capacity were correlated with the desiccation tolerance index of the studied species. The existence of a potential evolutionary trade-off between cell wall thickness and desiccation tolerance is rejected. The photosynthetic capacity reported for bryophytes is independent of elasticity and desiccation tolerance. Furthermore, the role of cell wall thickness in limiting CO_2 conductance would be overestimated under a scenario of high cell wall porosity for most bryophytes.

1 | INTRODUCTION

Desiccation tolerance is defined as the capacity to recover normal function after rehydration from a desiccated state of a minimum water potential of −100 MPa, equivalent to the loss of approximately 90% of the intracellular water (Gaff, 1997; Oliver et al., 2020). This has been considered a "primitive" trait (Oliver et al., 2005), because of the high frequency of this feature in the non-monophyletic descendants from the earliest branching events in the phylogeny of land plants, i.e. the bryophytes (Wood, 2007). It is generally accepted that desiccation tolerance was lost during early evolution of tracheophytes—remaining possibly in seeds, spores, and fern gametophytes (Ballesteros et al., 2020; López-Pozo, Ballesteros, et al., 2019; Watkins et al., 2007)—and that it was reacquired separately during land plant evolution for all tracheophyte lineages, except for gymnosperms (Farrant & Moore, 2011).

Despite different desiccation tolerance origins, several strategies have been shown to be in common for both bryophyte and tracheophyte desiccation tolerant (DT) species, possibly with the involvement of a seed-derived strategy for the latter (Farrant et al., 2020; Farrant & Moore, 2011; Oliver et al., 2010). An either constitutive or induced efficient antioxidant system or the expression of Late Embryogenesis Abundant (LEA) proteins in angiosperms and LEA-like rehydrins in bryophytes are two examples of this (Oliver et al., 2005).

The requirements of the cell wall for favoring desiccation tolerance have been also widely studied. Collapsed folded cell walls frequently occur when both "resurrection" plants (DT ferns and angiosperms) and bryophytes desiccate (Moore, Vicré-Gibouin, et al., 2008; Pressel et al., 2010; Proctor, 2001; Proctor et al., 2007; Shivaraj et al., 2018). This phenomenon has been related with specificities in the chemical composition of the cell wall (Moore, Farrant, & Driouich, 2008; Webb & Arnott, 1982) and it has been linked to the capacity to maintain ultrastructural organization and to avoid mechanical stress on cells during desiccation/rehydration cycles. Consequently, the bulk modulus of elasticity (ε) of leaves/shoots seems to be associated to desiccation tolerance for both bryophytes (Proctor et al., 1998) and resurrection plants (Nadal, Perera-Castro, et al., 2021). Cell wall thickness (T_{cw}) also seems to play a role in desiccation tolerance, although the mechanisms remain unclear. Hence, Nadal, Brodribb, et al. (2021) recently reported a generalized tendency of resurrection plants to present thicker cell walls compared with desiccation sensitive (DS) species of similar photosynthetic capacity. An intraspecific increase in T_{cw} has also been described as a response to desiccation stress in algae (Hoppert et al., 2004; Morison & Sheath, 1985). However, the relationship between ε or T_{cw} with a quantitative index for the degree of long-term desiccation tolerance of bryophytes has not been reported yet.

Both ε and T_{cw} have been linked with the photosynthetic capacity. T_{cw} is considered one of the main anatomical traits limiting CO_2 diffusion and responsible for the variability of mesophyll conductance of land plants (Evans et al., 2009; Gago et al., 2020; Peguero-Pina et al., 2017; Veromann-Jürgenson et al., 2020). Regarding elasticity, Nadal et al. (2018) reported a negative trade-off between net CO_2 assimilation rates (A_N) and ε for ferns and angiosperms, which included a few resurrection plants, so that species with a lower ε (higher elasticity) presented also high A_N through a still unclear mechanistic/evolutionary trade-off. In bryophytes, among other specific groups of plants, ε is not associated with their A_N, and the capacity to mobilize large amounts of water during dehydration (i.e. higher capacitance at full turgor) is not translated in higher rates of gas exchange (Perera-Castro, Nadal, & Flexas, 2020). In other words, if elasticity is hypothesized to be involved in the desiccation tolerance of bryophytes, it would not be a constraint for their photosynthetic capacity. On the contrary, very thick cell walls and low exposed chloroplast surface have been related to the low mesophyll conductance of bryophytes (Carriquí, Roig-Oliver, et al., 2019). In bryophytes, the combination of the thickest cell walls among the land plant phylogeny and the lowest photosynthetic rates (see compiled data of Flexas et al., 2021) have led to the hypothesis that the reduction of T_{cw} through the evolution of land plants is part of a potential trade-off between photosynthetic capacity and desiccation tolerance (Carriquí et al., 2015; Gago et al., 2019; Hanson et al., 2014).

Beyond this potential trade-off, the role of cell walls in limiting the photosynthetic capacity of bryophytes in still under debate. The low reported A_N of bryophytes seems to be due to CO_2 diffusion mainly limiting or co-limiting the biochemistry of the photosynthetic capacity (Carriquí, Roig-Oliver, et al., 2019; Perera-Castro, Waterman, et al., 2020). However, the anatomical modeling applied so far to bryophytes—and to any measured plant—assumes low values of effective porosity of cell walls, either constant or arbitrarily and negatively varying with T_{cw} (Evans et al., 2009; Terashima et al., 2006). Since the relationship between A_N and T_{cw} along the land plant's phylogeny is not linear, but asymptotic, with mosses presenting the thickest and lowest (but positive) A_N (Flexas et al., 2021), every unit of cell wall seems not to be as restrictive for CO_2 diffusion in bryophytes as it is in, e.g. angiosperms. This observation led us to suspect that a larger cell wall porosity could occur in bryophytes as compared with vascular plants. Not knowing the real porosity of the cell walls results in large uncertainties about the percent distribution of estimated anatomical limitations (Tomás et al., 2013, 2014; Tosens, Niinemets, Westoby, & Wright, 2012; Tosens et al., 2016; Lu et al., 2016; Han et al., 2018; Tosens & Laanisto, 2018; Carriquí, Roig-Oliver, et al., 2019, Carriquí, Douthe, et al., 2019).

The aims of the present study were to describe the physical factors related to the desiccation tolerance of poikilohydric species of bryophytes—mosses, liverworts, and hornworts—lycophytes (*Selaginella denticulata*) and ferns (*Hymenophyllum* spp.), especially those regarding cell wall properties, i.e. T_{cw} and ε, and to discuss their role as the potential drivers of an evolutionary trade-off between photosynthetic capacity and desiccation tolerance. Water relations, gas exchange, and anatomical traits were measured, as well as the weighed recovery of photosynthetic function after short/long-term desiccation/rehydration cycles as a quantitative index of desiccation tolerance.

2 | MATERIALS AND METHODS

2.1 | Plant materials and growing conditions

Sixteen species were analyzed in this study (Table 1): one hornwort, seven mosses, five liverworts, one lycophyte, and two filmy ferns (*Hymenophyllum* spp.). Species were collected in Mallorca (Balearic Islands), Tenerife (Canary Islands), La Rioja (Spain), Effeltrich (Germany), and Parque Katalapi (Puerto Montt, Chile). Specimens of some species (*P. purum*, *T. tamariscinum*, *P. undulatum*, *L. cruciata*, and *S. denticulata*) were grown in a moss greenhouse at the University of Balearic Island (UIB, Mallorca, Spain) for more than one year and they were part of the established UIB bryophytes collection before measurements. The rest of the species were measured immediately after collection within the next five days. Native substrate in perforate trays, daily watered with deionized water, was used for the long-term culturing of bryophytes. For gas exchange measurements, anatomical analysis, pressure–volume curves, and desiccation assays, samples were cleaned, and brown tissues were removed. Green, healthy thalli/shoots were incubated overnight in Petri dishes covered with wet tissues before measurements to avoid possible negative effects of the cutting (Wang et al., 2021). The studied specimen corresponded to some of those listed in Perera-Castro, Nadal, and Flexas (2020), for which net CO_2 assimilation rates were at 400 μmol CO_2 mol^{-1} air and some pressure–volume derived parameters were already reported.

TABLE 1 List of studied species, origin, and ecology/morphology/taxonomy information

Species	Phylum	Family	Morphology	Origin
Anthoceros agrestis (Paton) Damsholt	Anthocerotophyta	Anthocerotaceae	Thalloid	Tenerife
Fissidens serrulatus Brid.	Bryophyta	Fissidentaceae	Leafy	Tenerife
Plagiomnium undulatum (Hedwig) T. J. Koponen	Bryophyta	Mniaceae	Leafy	Mallorca[a]
Polytrichastrum formosum Hedw.	Bryophyta	Polytrichaceae	Leafy	Effeltrich
Polytrichum juniperinum Hedw.	Bryophyta	Polytrichaceae	Leafy	Tenerife
Pseudoscleropodium purum (Hedw.) M. Fleisch.	Bryophyta	Brachytheciaceae	Leafy	Mallorca[a]
Sphagnum palustre L.[b]	Bryophyta	Sphagnaceae	Leafy	La Rioja
Thuidium tamariscinum (Hedw.) Schimp.	Bryophyta	Thuidiaceae	Leafy	Mallorca[a]
Selaginella denticulata (L.) Spring	Lycophyta	Selaginellaceae	Leafy	Mallorca[a]
Durmortiera hirsuta (Sw.) Nees	Marchantiophyta	Marchantiaceae	Thalloid	Tenerife
Lunularia cruciata (L.) Dumort. ex Lindb.	Marchantiophyta	Lunulariaceae	Thalloid	Mallorca[a]
Pellia endiviifolia Dicks. Dum	Marchantiophyta	Pelliaceae	Thalloid	Tenerife
Porella canariensis (F.Weber) Underw.	Marchantiophyta	Porellaceae	Leafy	Tenerife
Saccogyna viticulosa (L.) Dumort.	Marchantiophyta	Geocalycaceae	Leafy	Tenerife
Hymenophyllum caudiculatum Mart.	Pteridophyta	Hymenophyllaceae	Leafy	Concepción (Chile)
Hymenophyllum dicranotrichum (C. Presl) Hook. ex Sadeb.	Pteridophyta	Hymenophyllaceae	Leafy	Concepción (Chile)

[a]Grown for more than 1 year in a moss greenhouse at University of Balearic Islands daily watered with deionized water at ambient temperature.
[b]Correspond to *Sphagnum* sp. of Perera-Castro, Nadal, and Flexas (2020).

2.2 | Long-term desiccation tolerance assay

In order to test the desiccation tolerance of the studied species, the "Falcon Test" method was modified after López-Pozo, Flexas, et al. (2019) as described in Perera-Castro et al. (2021) for bryophytes. Briefly, it is based on the capacity of the specimens to recover maximum quantum yield of PSII (F_v/F_m) when rehydrated after short/long storage in dried conditions (relative water content at equilibrium <1%–5%) inside 50 ml Falcon tubes with 12 g of silica gel with a relative humidity lower than 10% in equilibrium, which corresponds to a water potential of −310 MPa (Gaff & Oliver, 2013). F_v/F_m was measured with the fluorometer IMAGING-PAM (Heinz Walz GmbH) before and after the dehydration/rehydration cycle. The imaging of chlorophyll fluorescence allowed to average the F_v/F_m values of all pixels corresponding with plant tissue, using minimum fluorescence (F_0) image for selecting the area of interest.

The excess of interstitial water was removed from the full hydrated specimen by gently pressing them against a dry tissue. Hundred milligrams of fresh weight per sample and tube were used, resulting in a rate of drying of 62 mg g^{-1} dry weight per hour (López-Pozo, Flexas, et al., 2019). A thin net avoided direct contact of plant material with the silica gel. After 24 h, seven days, 14 days, and 30 days, samples ($n = 3$–4 independent samples per each period and species) were rehydrated by covering with wet tissues and stored in petri dishes for 24 h. The relative recovered F_v/F_m at each period of time (rF_v/F_{mi}, where i is the total days of desiccation) was calculated as.

$$rF_v/F_{mi} = \frac{F_v/F_{mi}}{F_v/F_{m0}}$$

where F_v/F_{m0} is the F_v/F_m measured before desiccation. In order to weight up recovery after longer times, the desiccation tolerance index (DTI) was calculated as:

$$\mathrm{DTI}(\%) = 100\frac{\Sigma(rF_v/F_{mi}\cdot i)}{\Sigma i}$$

This index was developed by using the strongest desiccant tested by López-Pozo, Flexas, et al. (2019), the silica gel, varying the length of dry state seeing the high percentage of bryophytes that fully recover F_v/F_m after 24 h of fast desiccation and rehydration. Thus, only species with values of DTI equal to 0 were considered fast desiccation sensitive (DS), while species with DTI > 0 were attributed qualitatively to fast desiccation tolerant species (DT).

2.3 | Pressure–volume curves

Six pressure–volume curves per species were performed by slowly air-drying full hydrated samples and alternately weighing and measuring its water potential by using a psychrometer (model WP4C, Decagon Device Inc.). The excel tool of Sack and Pasquet-Kok (2011) was used for delimiting the turgor loss point and calculating pressure–volume derived parameters. Turgid weight (TW) of each specimen was estimated as the x-intercept of leaf water potential (Ψ_{leaf}) versus fresh weight at any time on the curve (FW). Notice that the used method for calculating TW allows a reliable differentiation of their maximum internal water content (Perera-Castro, Nadal, &

Flexas, 2020), frequently problematic in bryophytes (e.g. Koster et al., 2010). Thus, relative water content (RWC) was calculated as RWC = 100 (FW − DW)/(TW − DW). DW is the dry constant weight and was obtained after keeping the samples at 70°C for 2–3 days. The point from which the Pressure–volume curve [$-1/\Psi_{leaf}$ − (100 − RWC)] became linear was considered the turgor loss point. RWC and Ψ_{leaf} measured at that point was obtained (RWC_{tlp} and π_{tlp}, respectively). The saturating water content (SWC) was calculated as SWC = (TW − DW)/DW.

Osmotic potential at full rehydration (π_o) was calculated as −1/y-intercept of the linear regression of the pressure–volume curve under turgor loss point. The bulk modulus of elasticity (ε) was calculated as the slope of pressure potential versus total RWC. Absolute leaf capacitance at full turgor (C_{ft}) was determined from the initial slope of the relationship between Ψ_{leaf} and RWC, and was normalized by leaf/shoot/thallus DW: C_{ft} = (TW − DW) ΔRWC/($\Delta\Psi_{leaf}$ DW). Capacitance at turgor loss point (C_{tlp}) was calculated as C_{ft} but for the relationship between Ψ_{leaf} and RWC for values below turgor loss point. The extracellular apoplastic fraction (a_f) was considered the fraction of water content when osmotic potential = −∞ and was calculated as x-intercept of the pressure–volume curve under turgor loss point. For the same samples used in pressure–volume curves and, when possible, gas exchange, shoot/thalli mass area (SMA) was calculated as the ratio of the projected shoot/thalli area and its DW.

2.4 | Gas exchange and chlorophyll fluorescence measurements

Gas exchange measurements were performed by using a GFS-3000 system coupled with an IMAGING-PAM fluorometer (Heinz Walz) and a custom-made moss cuvette consisting of a gasket affixed to a piece of thin polyester stocking fabric (illustrated as supplementary information in Perera-Castro, Nadal, & Flexas, 2020). CO_2 response curves of net CO_2 assimilation rate (A_N) were performed for six replicates of each species, except for *P. undulatum*, *Hymenophyllum* spp., and *S. palustre*, where only instantaneous A_N at 400 μmol CO_2 mol^{-1} air was determined due to logistic problems related with the handling of the samples during measurements. Relative humidity was kept at 75%–85%, blue irradiance (I) at saturation level (100–1000 μmol m^{-2} s^{-1}, depending on the species, tested previously with A_N–I curves), and air temperature in the gas exchange cuvette at 25°C. The flow rate within the chamber was 750 μmol s^{-1}. The concentration of CO_2 surrounding the sample inside chamber (C_a) was first set at 400 μmol mol^{-1}, then for CO_2-response curves C_a was decreased stepwise down to 50 μmol mol^{-1} and returned to its original value, followed by a stepwise increase up to 2000 μmol mol^{-1}. After each step of C_a, samples were removed from the chamber and placed again in the wet Petri dishes with deionized water for 2 min to avoid their desiccation during measurements, except in the case of *S. denticulata*, which was measured without the moss cuvette and with the base of the outside shoots and rhizoids under water. Most excessive external water was removed gently with a dry tissue before introducing the sample in the GFS chamber. In order to avoid the errors derived from CO_2 leakage in the parameterization of photosynthesis (Flexas et al., 2007), measurements of apparent net CO_2 assimilation at 200, 700, 1300, and 2000 μmol CO_2 mol^{-1} air were done for an empty moss cuvette before introducing the specimen. A_N and chlorophyll fluorescence (steady-state and maximum light-adapted fluorescence, F_s and F'_m, respectively) were recorded at steady-state conditions, when diffusional limitations due to external water were considered null and biochemistry was fully light-adapted (5–20 min). A_N was normalized to the measured thallus/shoot area. Light-adapted yield of PSII (ϕ_{PSII}) was calculated according to Genty et al. (1989): $\phi_{PSII} = (F'_m - F_s)/F'_m$. Electron transport rate was calculated from chlorophyll fluorescence (J_{FLU}) according to Krall and Edwards (1992): $J_{FLU} = \phi_{PSII}\, I\, \alpha\beta$, where $\alpha\beta$ is the product of absorbed quanta between PSI and PSII and was determined as 4/slope of the relationship between ϕ_{PSII} and ϕ_{CO2} ($[A_N + R_L]/I$) obtained by varying irradiance under non-photorespiratory conditions in an atmosphere containing <1% O_2 (Valentini et al., 1995). Light curves under non-photorespiratory conditions were measured after CO_2 curves and at 400 μmol CO_2 mol^{-1} air. Mitochondrial respiration under light condition (R_L) was calculated from the initial light-limited portion of the low-O_2-light curves as the negative intercept of the relationship between A_N and (ϕ_{PSII} I)/4 according to Yin et al. (2011). Mitochondrial respiration under dark conditions (R_D) at 400 μmol CO_2 mol^{-1} air were also measured after 10 min of darkness, except for *Hymenophyllum* spp.

2.5 | Anatomical analysis

Twelve out of the nineteen studied species were selected for anatomical analysis: *A. agrestis*, *F. serrulatus*, *L. cruciata*, *P. endiviifolia*, *P. undulatum*, *P. formosum*, *P. juniperinum*, *P. canariensis*, *P. purum*, *S. viticulosa*, *S. denticulata*, and *T. tamariscinum*. Three pieces of leaves/thalli/phyllidia of the same individuals on which gas exchange was performed were taken per species and fixed under vacuum with 4% glutaraldehyde and 2% paraformaldehyde in 0.1 M phosphate buffer (pH 7.2). Then, fixed fragments were washed three times in 0.1 M sodium cacodylate buffer (pH 7.2) with 5% sucrose, and stored overnight at 4°C in the same buffer. Afterwards, samples were incubated at 30°C for 2 h in a mixture (1:1) of 2% osmium tetroxide and 8% potassium ferrocyanide, followed by dehydration in a graded ethanol series. The dehydrated fragments were embedded in LR White resin (medium grade, London Resin Company Ltd.) and cured in an oven at 60°C for 48 h. Semi-thin (0.8 μm) and ultrathin (90 nm) transversal sections were obtained with an ultramicrotome and contrasted with 1% toluidine blue or Reynolds lead citrate solution (Reynolds, 1963), respectively. Photographs of the semi-thin sections were taken at ×200 and ×500 magnification with a light microscope (Olympus) and were photographed with a Moticam 3 (Motic Electric Group Co.). Contrasted ultra-thin sections were viewed at ×1500 and ×30 000 magnification using a transmission electron microscope (TEM H600, Hitachi). All images were analyzed using the software

ImageJ (Wayne Rasband/NIH). Thalli/phyllidia thickness (T_{leaf}), total length of cells and chloroplasts facing intercellular or external air spaces (L_m and L_c, respectively) and the volume fraction of intercellular air space (f_{ias}, only for *S. denticulata* and *L. cruciata*, assuming for the latter that chambers of fibrils were air-filled during gas exchange measurements) were measured from images obtained by light microscopy. Cell wall thickness (T_{cw}), chloroplast thickness (T_{chl}), and cytosol path length (L_{cyt}, from cell wall to chloroplast) were measured from TEM photographs (5–8 measurements per photo, 2–3 photos of different fields per replicate). Surface area of mesophyll cells or chloroplasts exposed to intercellular airspaces per unit leaf area (S_m and S_c, respectively) were calculated as described in Evans et al. (1994), applied for bryophytes by Carriquí, Roig-Oliver, et al. (2019):

$$S_m = \frac{L_m}{W} \cdot \gamma$$

$$S_c = \frac{L_c}{W} \cdot \gamma$$

where W is the width of the measured section (which covered the complete thickness of the thalli/phyllidia) and γ is the curvature correction factors from Thain (1983). γ was calculated to be 1.31–1.36 for most of the studied species (1.43 for *S. denticulata*), except for *P. purum*, whose tubular cell morphology was considered to be cylindrical without curvature effect ($\gamma = 1$).

2.6 | Mesophyll conductance calculations and limitations of photosynthesis

Mesophyll conductance (g_m) was calculated using two different methods: by curve-fitting method (g_{mCF}) and by anatomical modeling (g_{mANAT}).

2.6.1 | Curve-fitting method for calculating mesophyll conductance

The curve-fitting method is based on the calculation of the maximum carboxylation capacity (V_{cmax}), the maximum capacity for electron transport rate (J_{max}), the velocity for triose phosphate utilization (TPU), and g_m that best fit CO_2 curve data to the model of Farquhar et al. (Farquhar et al., 1980; Van Caemmerer & Evans, 1991, modified by Ethier & Livingston, 2004, and Sharkey et al., 2007, to include g_m). The excel tool of Sharkey et al. (Sharkey, 2016) was used for the fitting. The fitting was done for A_N–C_c curves, being C_c the concentration of CO_2 at the carboxylation site of Rubisco: $C_c = C_a - A_N/g_m$, in the case of bryophytes which lack stomata and intercellular airspaces, or $C_c = C_i - A_N/g_m$ in the case of *S. denticulata*, where C_i is the CO_2 concentration in the sub-stomatal cavity. In vitro Rubisco Michaelis–Menten constants for carboxylation (K_c) and oxygenation (K_o) and chloroplastic CO_2 photocompensation point (Γ^*) used for the curve fitting were obtained from averaged values for mosses, liverworts and lycophytes reported by Font and Galmés (2016) and Galmés et al. (2014; Table S1).

The relative mesophyll (l_m), stomatal (l_s), and biochemical (l_b) limitations to photosynthesis were calculated according to Grassi and Magnani (2005) with the modifications of Carriquí, Roig-Oliver, et al. (2019) for bryophytes:

$$l_s = \frac{g_{tot}/g_s \cdot \partial A_N/\partial C_c}{g_{tot} + \partial A_N/\partial C_c}$$

$$l_m = \frac{g_{tot}/g_m \cdot \partial A_N/\partial C_c}{g_{tot} + \partial A_N/\partial C_c}$$

$$l_b = \frac{g_{tot}}{g_{tot} + \partial A_N/\partial C_c}$$

where g_s is the stomatal conductance to CO_2 and g_{tot} is total conductance to CO_2 between leaf surface and carboxylation sites ($1/g_{tot} = 1/g_s + 1/g_m$). In bryophytes, $g_{tot} = g_{mCF}$.

2.6.2 | Anatomical modeling of mesophyll conductance

Values of g_{mANAT} were obtained by using the one-dimensional gas diffusion model of Niinemets and Reichstein (2003a, 2003b) as modified by Tomas et al. (2013) and Carriquí, Roig-Oliver, et al. (2019), where g_m is considered to be composited by gas phase conductance (g_{ias}, from substomatal cavities to outer surface of cell walls) and liquid phase conductance (g_{liq}, from outer surface of cell walls to chloroplasts):

$$g_{mANAT} = \frac{1}{\frac{1}{g_{ias}} + \frac{RT}{Hg_{liq}}}$$

where R is the gas constant (Pa m^3 K^{-1} mol^{-1}), T is the absolute temperature (K), and H is the Henry's lay constant (Pa m^3 mol^{-1}). For most bryophytes and leafy ferns, CO_2 resistance of the internal gas phase was considered zero ($1/g_{ias} = 0$), due to the lack of internal airspaces. The chambers of *L. cruciata* were assumed to be air-filled during gas exchange measurement and sample fixation for anatomy analysis, and the concentration of CO_2 (C_a) was assumed to be equal inside and outside the pore. For *L. cruciata* and *S. denticulata*, g_{ias} was calculated by average gas-phase thickness (ΔL_{ias}) and gas-phase porosity (f_{ias}):

$$g_{ias} = \frac{D_a f_{ias}}{\Delta L_{ias} \varsigma}$$

where ς is the diffusion path tortuosity (m m^{-1}) and D_a is the diffusion coefficient for CO_2 in the gas phase (1.51×10^{-5} m^2 s^{-1} at 25°C). ΔL_{ias} was calculated as half the mesophyll thickness. g_{liq} was calculated as:

$$g_{liq} = \frac{S_c}{\left(\frac{1}{g_{cw}} + \frac{1}{g_{pl}} + \frac{1}{g_{cyt}} + \frac{1}{g_{en}} + \frac{1}{g_{st}}\right)}$$

where g_{cw}, g_{pl}, g_{cyt}, g_{en}, and g_{st} are cell wall, plasmatic membrane, cytosol, chloroplast envelope and stroma conductance, respectively. g_{pl}

and g_{en} were assumed to be 0.0035 m s^{-1} (Evans et al., 1994). The rest of determinants of the liquid-phase diffusion pathway were calculated as:

$$g_i = \frac{r_{f,i} D_w p_i}{\Delta L_i}$$

where *i* stands either for cell wall, cytosol, or stroma conductance. D_w is the aqueous phase diffusion coefficient for CO_2 (1.79×10^{-9} m^2 s^{-1} at 25°C). The dimensionless factor $r_{f,i}$ accounts for the reduction of D_w compared with free diffusion in water, and assumed 1.0 for cell walls (Rondeau-Mouro et al., 2008) and 0.3 for cytosol and stroma (Niinemets & Reichstein, 2003a; Niinemets & Reichstein, 2003b). ΔL_i (m) is the diffusion path length in the corresponding component of the diffusion pathway:

$$\Delta L_{cw} = T_{cw}$$

$$\Delta L_{cyt} = T_{cyt}$$

$$\Delta L_{st} = \frac{T_{chl}}{2}$$

p_i (m^3 m^{-3}) is the effective porosity of the diffusion pathway, assumed to be 1 for cytosol and stroma components. Cell wall porosity (p_{cw}) was assumed to be 0.1 (Tomás et al., 2014), one of the highest constant values assumed for calculating g_{mANAT}. Cell wall porosity was also calculated by allowing g_{mANAT} to match g_{mCF} (then termed p_{CF}). The percentage of contribution to g_{liq} was calculated for each component of the liquid-phase diffusion pathway as:

$$l_i(\%) = 100 \frac{g_{liq}}{g_{cw} S_c}$$

where *i* in this case stands either for cell wall, cytosol, stroma, plasmatic membrane or chloroplast envelope. The effect of a possible CO_2 concentration mechanism in *A. agrestis* due to the presence of pyrenoids (Smith & Griffiths, 1996) was not considered since x-intercept of A_N–C_a curves was 48.7 ± 6.8 µmol CO_2 mol^{-1}, not lower than that of other bryophytes lacking pyrenoids like *P. juniperinum* (42.4 ± 10.7 µmol CO_2 mol^{-1}) or *P. formosum* (29.6 ± 5.3 µmol CO_2 mol^{-1}).

2.7 | Statistical analysis

All analyses were performed using the R statistical software (R Core Team, 2016). Linear regressions were used to test the relationship between mesophyll conductance parameters calculated with curve-fitting and anatomical modeling, as well as for testing the relation between desiccation tolerance index and anatomical, pressure–volume and gas exchange-derived parameters. Non-lineal model (power or logarithmic function) was also fitted to the relationship between CO_2 assimilation rates and anatomical derived parameters, as well as to the relationship among pressure volume derived parameters. In those cases, averaged values per species were used. Differences in pressure–volume derived parameters between DT and DS species and differences between percentages of biochemical versus mesophyll limitation to photosynthesis were tested by Mann–Whitney *U* test, as well as differences between the measured pressure–volume derived parameters and those reported for ferns and angiosperms (Bartlett et al., 2012; Nadal et al., 2018; Shrestha et al., 2007) and for bryophytes (Cruz de Carvalho et al., 2015; Hájek & Beckett, 2008). The packages used were "plyr" (Wickham, 2011), "ggplot2" (Wickham, 2016), "reshape2" (Wickham, 2007), and "corrplot" (Wei et al., 2017).

3 | RESULTS

3.1 | Long-term desiccation tolerance

The long-term desiccation assay revealed a wide range of tolerances, from a DTI of 80% for the leafy liverwort *P. canariensis* to a null capacity of recovery of F_v/F_m for all thalloid species, the leafy liverwort *S. viticulosa* and the moss *S. palustre* (Figure 1). The lycophyte *S. denticulata* and the filmy ferns *H. caudiculatum* and *H. dicranotrichum*

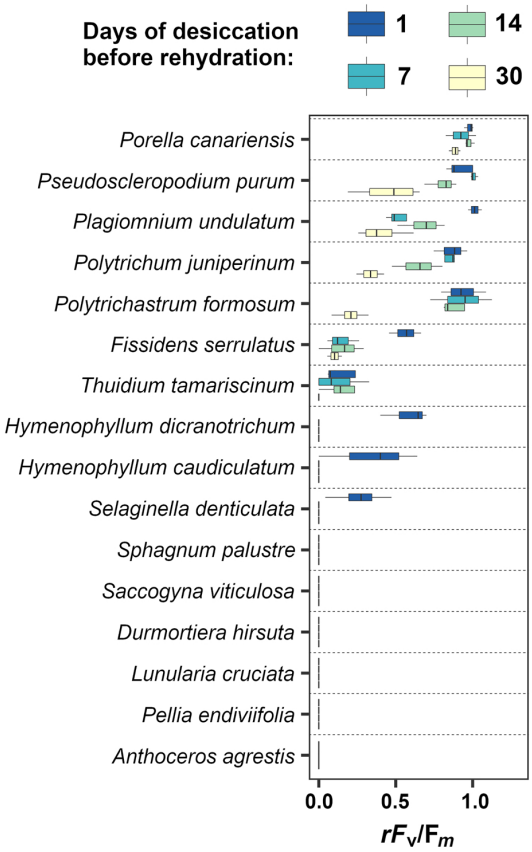

FIGURE 1 Recovery of F_v/F_m (i.e. the ratio between final and initial F_v/F_m values after and before desiccation, respectively) of the studied species after 24 h of rehydration of dry samples kept in silica gel for 1, 7, 14, or 30 days. Boxplots with defaults settings of "ggplot"

showed a recovery capacity of 26.5, 34.6, and 58.1% of F_v/F_m, respectively, if the desiccation period did not exceed 24 h.

3.2 | Water relations

All the parameters derived from water relation analyses are shown in Table S2. The water potential at turgor loss point (π_{tlp}) was determined mostly by osmotic potential at full turgor (π_o) in both DT and DS species (Figure S2A, $P < 0.001$, $R^2 = 0.645$) and, to some extent, by bulk modulus of elasticity (ε; Figure S2B, $P = 0.003$, $R^2 = 0.459$). The x-intercept of the π_{tlp}–π_o relationship of bryophytes and *S. denticulata* was significantly different for the regression reported for ferns and angiosperms (Figure 2A), so that the studied species required higher values of π_o (less negative) than the reported vascular plants to achieve the same π_{tlp} (in average, 0.47 MPa of difference). The measured bulk modulus of elasticity for bryophytes and *S. denticulata* ranged between 0.68 and 6.4 MPa, values significantly lower than compiled data of vascular plants ($P < 0.001$ for the complete meta-analysis of Bartlett et al., 2012, plus data from Shrestha et al., 2007, and Nadal et al., 2018). Those low ε values corresponded to low RWC_{tlp}, resulting in a logarithmic RWC_{tlp}–ε relationship for all land plants plotted together (Figure 2B).

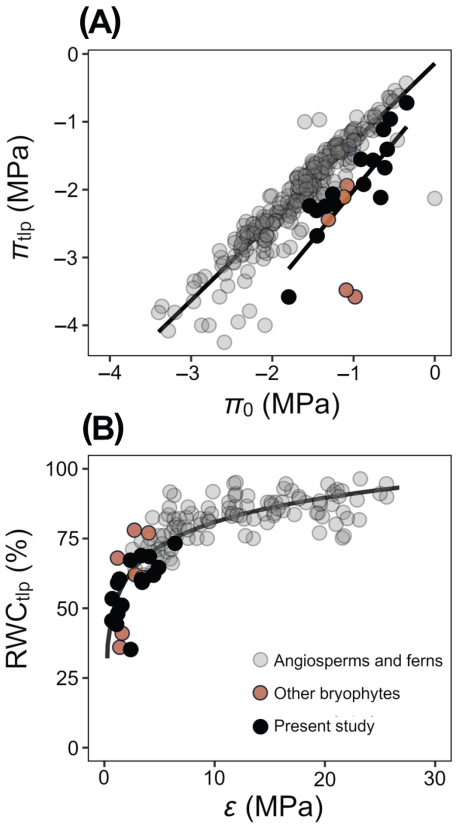

FIGURE 2 Contextualization of some pressure–volume derived parameters of bryophytes and *S. denticulata* of the present study in the angiosperms and ferns reported values of Nadal et al. (2018), Shrestha et al. (2007), and compiled data of Bartlett et al. (2012), as well as in the bryophytes reported values of Hájek and Beckett (2008) and Cruz de Carvalho et al. (2015). (A) Relationship between osmotic potential (π_o) and water potential at turgor loss point (π_{tlp}) for tracheophytes and presented data ($P = 0.016$ for differences in intercept; slope non-significatively different, $P = 0.135$). (B) Relationship between bulk modulus of elasticity (ε) and relative water content at turgor loss point (RWC_{tlp}; $P < 0.001$ for the logarithmic relationship: $RWC_{tlp} = 28.9 \log10(\varepsilon) + 51.8$). Data points are mean values of each reported species, except for values of Shrestha et al. (2007) of panel (B), which correspond to undetermined individuals

3.3 | Diffusional limitation to photosynthesis

Gas exchange-derived parameters are shown in Table S3. The obtained A_N–C_c curves are shown for each species in Figure S2. *P. juniperinum* and *P. formosum* presented the highest photosynthetic capacity, with the highest values of V_{cmax} (26.8 ± 3.8 and 22.9 ± 1.1 μmol m^{-2} s^{-1}, respectively, mean ± SE) and J_{max} (39.6 ± 2.7 and 27.6 ± 2.3 μmol m^{-2} s^{-1}, respectively). Besides *Polytrichum* species, most of the studied bryophytes (63%) showed values of V_{cmax} and J_{max} below 5.6 and 7.2 μmol m^{-2} s^{-1}, respectively, being the leafy liverworts *S. viticulosa* and *P. canariensis* and the moss *F. serrulatus* the species with the lowest averaged photosynthetic capacities, i.e. V_{cmax}

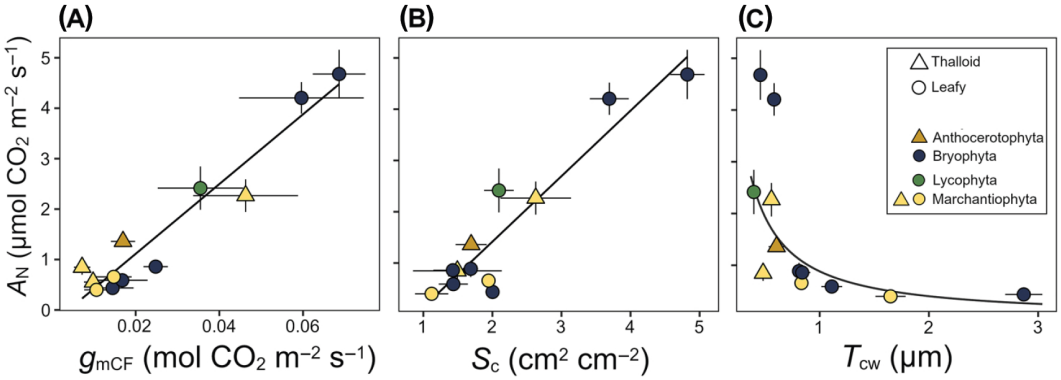

FIGURE 3 Anatomical determinants of net CO_2 assimilation rate (A_N). Relationship between A_N and (A) mesophyll conductance calculated though curve-fitting method (g_{mCF}, $P < 0.001$, $r^2 = 0.925$), (B) surface area of chloroplasts exposed to intercellular airspaces per unit leaf area (S_c, $P < 0.001$, $r^2 = 0.877$), and (C) thickness of cell wall (T_{cw}, $P < 0.001$, $r^2 = 0.680$ for the power function $A_N = 0.88\ T_{cw}^{-1.13}$). Data points are mean ± SE

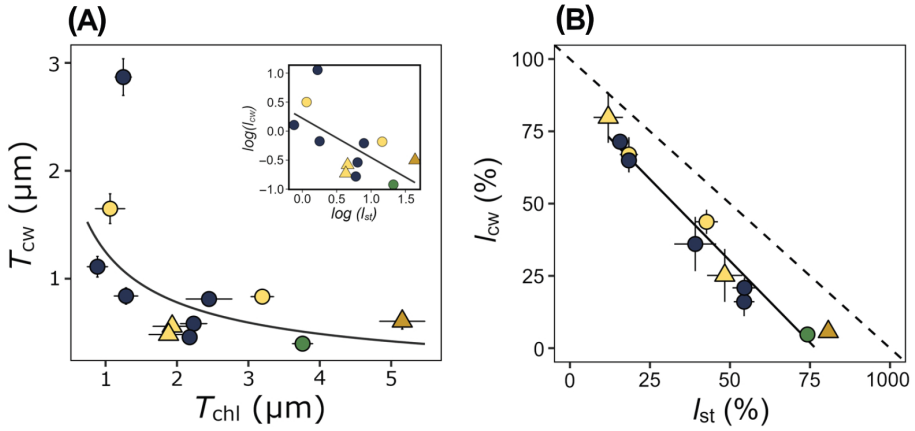

FIGURE 4 Balance between the morphology of cell wall and chloroplast. (A) Non-linear relationship between thickness of chloroplast (T_{chl}) and thickness of cell wall (T_{cw}). Line indicates power function: $T_{cw} = 1.24\ T_{chl}^{-0.677}$ ($P = 0.053$). Inset graph indicate logarithmic T_{cw}–T_{chl} relationship ($P = 0.030$). (B) Relationship between percentage of anatomical limitation to liquid component of mesophyll conductance of stroma (l_{st}) and cell wall (l_{cw}) with a porosity calculated by adjusting g_{mANAT} to g_{mCF} ($P < 0.001$ for linear regressions). See Figure 3 for legend

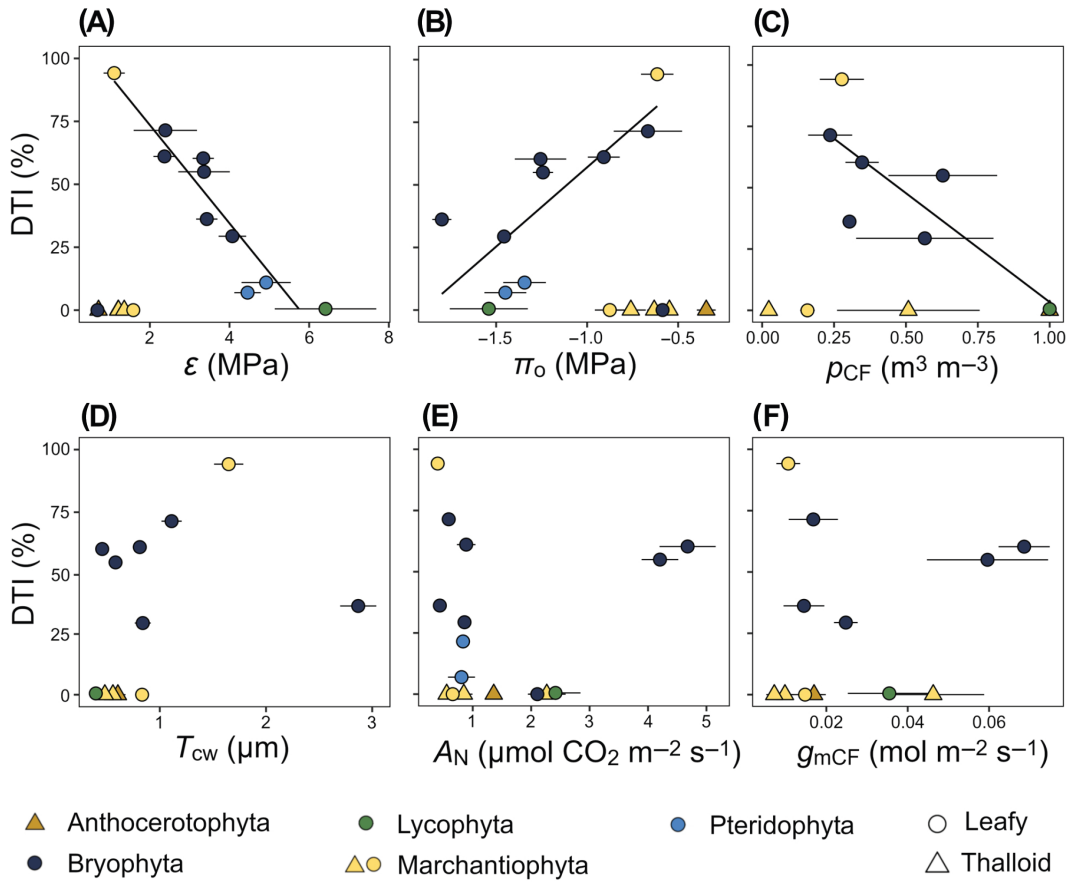

FIGURE 5 Physiological and morphological determinants of desiccation tolerance. (A) Relationship between desiccation tolerance index (DTI) and bulk modulus of elasticity (ε, $P < 0.001$), (B) osmotic potential (π_o, $P = 0.004$), (C) porosity calculated from g_{mANAT} adjusted to g_{mCF} (p_{CF}, $P = 0.032$), (D) thickness of cell wall (T_{cw}), (E) net CO_2 assimilation rate at 400 µmol mol^{-1} of external CO_2 (A_N), and (F) mesophyll conductance by curve-fitting method (g_{mCF}). Lines indicate regressions for desiccation tolerant species "sensu this study," i.e. all species with positive values of DTI. Data points indicate mean ± SE

below 4.5 μmol m^{-2} s^{-1} and J_{max} below 5.3 μmol m^{-2} s^{-1}. The correlation between J_{max} obtained by the curve-fitting method and J_{FLU} calculated by chlorophyll fluorescence was significant ($P = 0.005$, $R^2 = 0.555$, Figure S3), with only two species—*S. denticulata* and *L. cruciata*—with J_{FLU} values 2.4- and 1.9-fold higher than J_{max}. Biochemical limitation was significantly larger than diffusional limitation in all studied species (Table S4).

Values for the most relevant parameters measured for the anatomical model are shown in Table S5. A_N was highly and linearly correlated with g_{mCF} and S_c (Figure 3A,B), as well as with T_{cw} in a non-linearly way (Figure 3C). S_m were lower than 3.7 cm^2 cm^{-2} for most of the studied species, only higher in species with f_{ias} resulted from air-filled mesophyll or ventilated thallus—*S. denticulata* and *L. cruciata* (9.4 ± 1.0 and 6.6 ± 0.3 cm^2 cm^{-2}, respectively)—or lamellae—*P. formosum* and *P juniperinum* (10.3 ± 0.9 and 13.8 ± 0.3 cm^2 cm^{-2}, respectively). S_c and S_m were highly correlated ($P < 0.001$, $R^2 = 0.816$, regression not shown), with chloroplasts occupying on average 45% of the air facing surface. g_{mCF}/S_c and T_{cw} were not correlated significantly ($P = 0.186$, data not shown).

Mesophyll conductance calculated using the anatomical model (g_{mANAT}) was correlated with g_{mCF} (Figure S4, $P < 0.0001$), being g_{mCF} 1.7-fold higher than g_{mANAT}, except for the liverwort *P. endiviifolia*. When effective porosity was calculated so that g_{mANAT} matched g_{mCF} (p_{CF}), values higher than 0.3 m^3 m^{-3} were obtained for most of the studied species (Table S5). g_{mANAT} could match g_{mCF} in *A. agrestis* and *S. denticulata* only using unrealistic values of effective porosity higher than 1.

T_{cw} varied between 0.39 (for *S. denticulata*) and 2.86 μm (for *F. serrulatus*) and was non-linearly correlated with T_{chl} (Figure 4A, $P = 0.030$ for the logarithmic relationship, $P = 0.053$ for power function), so that species with the thickest cell walls also presented the thinnest chloroplasts (*F. serrulatus*, *P. purum*, and *P. canariensis*). The percentages of limitation to the liquid components of mesophyll conductance of stroma (l_{st}) and cell wall (l_{cw}) were also negatively correlated (Figure 4B). When porosity was estimated by adjusting g_{mANAT} to g_{mCF}—, l_{cw} was lower than 43% in favor of l_{st}, except for the species with thickest cell walls (*F. serrulatus* and *P. purum*) or with low p_{CF} (*P. endiviifolia*, with a $p_{CF} = 0.023 \pm 0.008$ m^3 m^{-3}). The variation of the percentages of limitation of all the components of the diffusion pathway considered for the anatomical model of mesophyll conductance are shown in Table S6 for constant and variable porosity.

3.4 | Factors related to desiccation tolerance

For DT species as defined in this study, i.e. species with DTI > 0, that index was negatively correlated with ε (Figure 5A, $P < 0.001$), that is, the largest long-term desiccation tolerance was observed in those DT species with more elastic tissues. DS species presented low values of ε (<0.2 MPa, elastic tissues) despite their null capacity to recover from desiccation. Something similar occurred for osmotic potential, which was positively correlated with DTI only for DT species (Figure 5B, $P = 0.004$). DTI was also negatively correlated with p_{CF} for DT species (Figure 5C, $P = 0.032$). Neither T_{cw} nor A_N or g_{mCF} were correlated with DTI (Figure 5D–F). a_f and C_{ft} were not correlated with long-term desiccation tolerance (data not shown), although their absolute values were significantly different for DT and DS species (Figure S5), so that on average DT species presented a_f values 3-fold higher than DS species and C_{ft} values 48% lower than DS ones.

4 | DISCUSSION

4.1 | Water relations and cell wall features as promoters of desiccation tolerance

The long-term fast desiccation/rehydration assay allowed the calculation of a quantitative index of desiccation tolerance (DTI). Our data show that DTI was mostly correlated with the bulk modulus of elasticity and osmotic potential at full turgor only in DT species (Figure 5A,B). All studied thalloid liverworts, the hornwort *A. agrestis*, the moss *S. palustre* and the leafy liverwort *S. viticulosa* experienced a complete inhibition of F_v/F_m for the shortest tested period of the fast desiccation applied in our study (24 h). For softer desiccation treatments—lower rate and depth of drying, especially in hardened individuals by previous abscisic acid treatments—some of these species have shown some recovery of F_v/F_m after rehydration (Pence et al., 2005; Pressel et al., 2009). All these sensitive species showed high elasticity, suggesting that elasticity is not the last determinant of tolerance, but still it is a compulsory requirement for bryophytes to tolerate the mechanical stress suffered after desiccation during longer periods. Low elasticity seems to be a generalized characteristic of bryophytes (Beckett, 1997; Proctor et al., 1998; Proctor, 1999; Hájek & Beckett, 2008; Cruz de Carvalho et al., 2015; notice that different methods for calculating ε were used in those studies), only emulated by some grasses and crops (Bartlett et al., 2012; Nadal et al., 2018). On the contrary, the values of π_o and π_{tlp} measured for bryophytes in this study (between −0.7 and −3.5 MPa, and −1.7 and 0.3 MPa, respectively) are more frequently found in angiosperms (Figure 2 for the contextualization of π_o–π_{tlp} and RWC_{tlp}–ε relationship of the present study in reported values for tracheophytes). In their meta-analysis, Bartlett et al. (2012) showed the association of low π_o or π_{tlp} (more negative values) with arid ecosystems and, therefore, with drought tolerance, placing ε and RWC_{tlp} into a secondary role. Our study demonstrates that the contrary occurs in bryophytes and possibly also in DT lycophytes and filmy ferns, with elasticity (i.e. low ε) being the only parameter highly correlated with a desiccation tolerance index, while absolute values of π_o and therefore π_{tlp}, only increase with rigidity. The high elasticity of bryophytes may explain their position in the π_{tlp}–π_o relationship and their low values of RWC_{tlp} according to the equations presented by Bartlett et al. (2012) defining the relationships among pressure–volume parameters. The concurrence of a possible mechanism of incompatibility between ε and π_o in bryophytes is not clear. The elasticity of cell walls in this group of plants may be mainly dependent of their chemical composition, which includes a higher accumulation of callose (Popper, 2008; Popper et al., 2011; Popper & Fry, 2003). Question arises as to whether the osmolytes that provoke the increase

of absolute values of π_o are also involved in making the tissues of the studied species more rigid, maybe not so clearly evidenced in tracheophytes (see correlations between ε and π_o of Zhang, 1998, Shrestha et al., 2007, and Bartlett et al., 2012) due to the role of additional structures in the determination of elasticity—for instance, thickened cuticles, lignified epidermal cells, fiber bundles, and the presence of sclereids (Salleo & Gullo, 1990).

Curiously, the effective porosity estimated by adjusting g_{mANAT} and g_{mCF} was significantly correlated with the DTI in DT species, but the thickness of cell wall was not (Figure 5C,D). As introduced, the high values of p_{CF} (>0.3 m^3 m^{-3} for most of the studied species) compared with the ones assumed for vascular plants (<0.1 m^3 m^{-3}, Tomás et al., 2013, 2014; Tosens, Niinemets, Vislap, et al., 2012, Tosens, Niinemets, Westoby, & Wright, 2012, Tosens et al., 2016; but see also Nobel, 1991) is consistent with the position of bryophytes in the asymptotic A_N–T_{cw} relationship. Furthermore, high p_{CF} may explain why the suggested link between T_{cw} and tissue rigidity for tracheophytes (Peguero-Pina et al., 2017) seems not to apply for the studied bryophytes. Nadal, Brodribb, et al. (2021) have also observed variations in ε associated to DT and DS fronds of the fern *Anemia caffrorum* independent of the T_{cw}, which was invariable. We recognize that the effective porosity calculated in our study could be overestimated due to the effect of additional biochemical enhancers of mesophyll conductance, i.e. carbonic anhydrases and aquaporins (reviewed by Gago et al., 2020), which could explain p_{CF} values >1 m^3 m^{-3}. Assuming that this possible underestimation is constant among studied species, our data suggest that having less porous cell walls seemed to be more relevant than their thickness for long-term desiccation tolerance in bryophytes and maybe lycophytes. We hypothesize that the less porous cell walls of DT species (p_{CF} = 0.27 m^3 m^{-3} for *P. canariensis* and 0.18 for *P. purum*) may evade penetration of digestive enzymes of microorganisms and enhance resistance to mineralization when desiccated. Both low nitrogen concentration and the presence of phenolic compounds have been pointed out as responsible for the low rates of decomposition of bryophytes as compared with tracheophytes (Scheffer et al., 2001; Turetsky, 2003). Perhaps, porosities of vascular plants have less interspecific variability and then an increase of T_{cw} and/or a decrease of nitrogen concentration are the only factors that resurrection plants can do for surviving desiccation periods, explaining their lower A_N/T_{cw} ratio (Nadal, Perera-Castro, et al., 2021).

Beyond T_{cw}, there must exist a direct relation between effective porosity, apoplastic fraction (or volume of apoplastic water), and the volume of total cell walls. In future studies, the combination of pressure volume curves and the deconstruction of 3D cell wall volume though the new X-ray microscanning technology (Théroux-Rancourt et al., 2020) would allow direct measurements of cell wall effective porosities and shed light about their role in desiccation tolerance and mineralization.

4.2 | Role of cell walls in limiting photosynthetic capacity of bryophytes

Independently of the role of effective porosity in determining desiccation tolerance, both A_N and T_{cw} were unrelated to DTI for the studied species. Surely, inherent variations in phyllids/thalli structure are defining g_m and photosynthetic capacity in bryophytes, as can be evidenced by the correlation between g_m modeled from anatomy and gas exchange (Figure S4). Among the measured anatomical traits, the present study evidences a clear dominance of S_c above T_{cw} in determining photosynthetic capacity of bryophytes and *S. denticulata* (Figure 3) in line with data reported by Carriquí, Roig-Oliver, et al. (2019) for bryophytes and lycophytes but contrary to the meta-analysis of Flexas et al. (2021) pooling bryophytes and tracheophytes. These discrepancies among anatomical determinants of photosynthesis along phylogeny, together with the null relationship between A_N or g_{mCF} and DTI reported in the present study, suggest that the evolutionary trade-off between photosynthetic capacity and desiccation tolerance proposed by Hanson et al. (2014) and Carriquí et al. (2015) is not based on a direct common mechanistic constrain related with T_{cw}.

Furthermore, the percentage of limitation of the liquid phase of mesophyll conductance due to cell wall (l_{cw}) was below 43% in most species when forcing $p_{cw} = p_{CF}$, resulting in increased estimated limitation due to the chloroplast stroma (Figure 4B). A trade-off between chloroplast and cell wall thickness was observed for the studied species (Figure 4A). While a similar relationship has been also established in some vascular plants (Tosens, Niinemets, Westoby, & Wright, 2012), a multispecies compiled dataset has instead shown a positive lineal correlation between them (Ren et al., 2019), which seem to be contradictory with the idea suggested by Tosens, Niinemets, Westoby, and Wright (2012) that species with thicker mesophyll cell wall resistance may be evolutionary constrained to reduce the diffusion pathway in chloroplast and stroma resistance. The advantages of bryophytes with thinner cell walls in presenting thicker chloroplasts are not clear. Since light harvesting capacity is restricted in this group of plants due to their morphology—phyllidia mostly unistratose and with light harvesting and chlorophyll concentration depending mostly on canopy structure (Wang et al., 2016)—, thicker chloroplasts would enhance chlorophyll and Rubisco concentration per unit area (Li et al., 2013), as well as light absorbance. The positive effects of enhancing light harvesting by increasing T_{chl} must be more relevant than the negative effects of increasing stroma resistance in species with the thinnest cell walls and low S_c.

In addition to the possible balanced role of cell wall and chloroplast size in determining mesophyll conductance in a scenario of high p_{cw}, photosynthesis was mainly limited by biochemistry rather than mesophyll conductance (Table S4). This is in contrast with previous report by Carriquí, Roig-Oliver, et al. (2019), who showed that mesophyll conductance limitation was the most limiting for photosynthesis in bryophytes. This apparent discrepancy could be due either to the fact that different species were analyzed in the two studies, but also to the fact that limitation analysis in Carriquí, Roig-Oliver, et al. (2019) were based on different methodology for estimating g_m. Such discrepancies reveal uncertainty as for considering g_m as the main ruler of photosynthetic capacity of bryophytes and need to be analyzed in depth in the near future. Despite these specific discrepancies, the results of the present study still confirm some conclusions of Carriquí,

Roig-Oliver, et al. (2019), i.e. (a) g_m is very low in bryophytes as compared with tracheophytes, and (b) it significantly contributes to limit their photosynthesis, which results in a very strong linear dependency of A_N on g_{mCF} (Figure 3A).

5 | CONCLUSIONS

In conclusion, elasticity is a common feature that favors desiccation tolerance beyond osmotic potential in bryophytes, the lycophyte *S. denticulata*, and filmy ferns, although it is not exclusive of desiccation tolerant species. In addition, less porous cell walls seem to be more relevant for enhancing desiccation tolerance than the increase of T_{cw} within the studied species, which suggests that the distinctive features of cell wall (generally thick cell walls possibly with high porosity) are not involved in the generalized desiccation tolerance reported for this group of plants. The role of T_{cw} in constraining the evolutionary tendency of decreasing desiccation tolerance along phylogeny of land plants, from the early branched group of bryophytes to the more recently diverged angiosperms, is rejected, since within bryophytes thick cell walls and low A_N does not correspond with higher tolerance to desiccation. Furthermore, our data evidence that the contribution of the cell walls to limiting mesophyll conductance is balanced with the thickness of stroma and, therefore, with chloroplast size, in the scenario of a high cell wall porosity estimated here. This observation, together with the high linear correlation between S_c and A_N suggest that T_{cw} is not only irrelevant for desiccation tolerance, but possibly also less relevant than previously thought for constraining photosynthetic capacity of bryophytes.

ACKNOWLEDGMENTS

This work was supported by the Ministerio de Ciencia, Innovación y Universidades (MCIU, Spain) and the ERDF (FEDER) [PGC2018-093824-B-C41] and the Ministerio de Educación, Cultura y Deporte (MECD, Spain), predoctoral fellowship [FPU-02054] awarded to AVP-C. We are grateful to Dr Ana Losada for identifying some of the studied mosses, and to Dr. Ferran Hierro and Dr Maria Pocovi for technical support during microscopic analyses. We thank Dr Néstor Fernández-Del-Saz and Dr Rafael Coopman for their support in species collection.

AUTHOR CONTRIBUTION

Alicia V. Perera-Castro and Jaume Flexas designed the study. Alicia V. Perera-Castro conducted the experiments, performed the analysis and wrote the first draft of the manuscript. Both authors contributed to the following and final versions of the manuscript.

DATA AVAILABILITY STATEMENT

The data that support the findings of this study are available in the supplementary material of this article and from the corresponding author, Alicia V. Perera-Castro, upon reasonable request.

ORCID

Alicia V. Perera-Castro https://orcid.org/0000-0001-8451-6052
Jaume Flexas https://orcid.org/0000-0002-3069-175X

REFERENCES

Ballesteros, D., Pritchard, H.W. & Walters, C. (2020) Dry architecture: towards the understanding of the variation of longevity in desiccation-tolerant germplasm. *Seed Science Research*, 30(2), 142–155.

Bartlett, M.K., Scoffoni, C. & Sack, L. (2012) The determinants of leaf turgor loss point and prediction of drought tolerance of species and biomes: a global meta-analysis. *Ecology Letters*, 15(5), 393–405.

Beckett, R.P. (1997) Pressure–volume analysis of a range of poikilohydric plants implies the existence of negative turgor in vegetative cells. *Annals of Botany*, 79(2), 145–152.

Carriquí, M., Cabrera, H.M., Conesa, M.À., Coopman, R.E., Douthe, C., Gago, J. et al. (2015) Diffusional limitations explain the lower photosynthetic capacity of ferns as compared with angiosperms in a common garden study. *Plant, Cell & Environment*, 38(3), 448–460.

Carriquí, M., Douthe, C., Molins, A. & Flexas, J. (2019) Leaf anatomy does not explain apparent short-term responses of mesophyll conductance to light and CO_2 in tobacco. *Physiologia Plantarum*, 165(3), 604–618.

Carriquí, M., Roig-Oliver, M., Brodribb, T.J., Coopman, R., Gill, W., Mark, K. et al. (2019) Anatomical constraints to nonstomatal diffusion conductance and photosynthesis in lycophytes and bryophytes. *New Phytologist*, 222(3), 1256–1270.

Cruz de Carvalho, R., da Silva, A.B., Branquinho, C. & da Silva, J.M. (2015) Influence of dehydration rate on cell sucrose and water relations parameters in an inducible desiccation tolerant aquatic bryophyte. *Environmental and Experimental Botany*, 120, 18–22.

Ethier, G.J. & Livingston, N.J. (2004) On the need to incorporate sensitivity to CO_2 transfer conductance into the Farquhar–von Caemmerer–Berry leaf photosynthesis model. *Plant, Cell & Environment*, 27(2), 137–153.

Evans, J.R., Caemmerer, S.V., Setchell, B.A. & Hudson, G.S. (1994) The relationship between CO_2 transfer conductance and leaf anatomy in transgenic tobacco with a reduced content of rubisco. *Functional Plant Biology*, 21(4), 475–495.

Evans, J.R., Kaldenhoff, R., Genty, B. & Terashima, I. (2009) Resistances along the CO_2 diffusion pathway inside leaves. *Journal of Experimental Botany*, 60(8), 2235–2248.

Farquhar, G.D., von Caemmerer, S.V. & Berry, J.A. (1980) A biochemical model of photosynthetic CO_2 assimilation in leaves of C_3 species. *Planta*, 149(1), 78–90.

Farrant, J.M. & Moore, J.P. (2011) Programming desiccation-tolerance: from plants to seeds to resurrection plants. *Current Opinion in Plant Biology*, 14(3), 340–345.

Farrant, J.M., Moore, J.P. & Hilhorst, H.W. (2020) Unifying insights into the desiccation tolerance mechanisms of resurrection plants and seeds. *Frontiers in Plant Science*, 11, 1089.

Flexas, J., Clemente-Moreno, M.J., Bota, J., Brodribb, T.J., Gago, J., Mizokami, Y. et al. (2021) Cell wall thickness and composition are involved in photosynthetic limitation. *Journal of Experimental Botany*, 72(11), 3971–3986.

Flexas, J., Díaz-Espejo, A., Berry, J.A., Cifre, J., Galmés, J., Kaldenhoff, R. et al. (2007) Analysis of leakage in IRGA's leaf chambers of open gas exchange systems: quantification and its effects in photosynthesis parameterization. *Journal of Experimental Botany*, 58(6), 1533–1543.

Font, M. & Galmés, J. (2016) Temperature response of in vitro Rubisco kinetics in bryophytes and ferns [Poster]. In: 17th International Congress on Photosynthesis Research, Maastricht.

Gaff, D.F. (1997) Mechanisms of desiccation tolerance in resurrection vascular plants. In: Basra, A.S. & Basra, R.K. (Eds.) *Mechanisms of environmental stress resistance in plants*. Amsterdam, The Netherlands: Harwood Academic Publishers, pp. 43–58.

Gaff, D.F. & Oliver, M. (2013) The evolution of desiccation tolerance in angiosperm plants: a rare yet common phenomenon. *Functional Plant Biology*, 40(4), 315–328.

Gago, J., Carriquí, M., Nadal, M., Clemente-Moreno, M.J., Coopman, R.E., Fernie, A.R. et al. (2019) Photosynthesis optimized across land plant phylogeny. *Trends in Plant Science*, 24(10), 947–958.

Gago, J., Daloso, D.M., Carriquí, M., Nadal, M., Morales, M., Araújo, W.L. et al. (2020) The photosynthesis game is in the "inter-play": mechanisms underlying CO_2 diffusion in leaves. *Environmental and Experimental Botany*, 178, 104174.

Galmés, J., Kapralov, M.V., Andralojc, P.J., Conesa, M.À., Keys, A.J., Parry, M.A. et al. (2014) Expanding knowledge of the rubisco kinetics variability in plant species: environmental and evolutionary trends. *Plant, Cell & Environment*, 37(9), 1989–2001.

Genty, B., Briantais, J.M. & Baker, N.R. (1989) The relationship between the quantum yield of photosynthetic electron transport and quenching of chlorophyll fluorescence. *Biochimica et Biophysica Acta (BBA)-General Subjects*, 990(1), 87–92.

Grassi, G. & Magnani, F. (2005) Stomatal, mesophyll conductance and biochemical limitations to photosynthesis as affected by drought and leaf ontogeny in ash and oak trees. *Plant, Cell & Environment*, 28(7), 834–849.

Hájek, T. & Beckett, R.P. (2008) Effect of water content components on desiccation and recovery in *Sphagnum* mosses. *Annals of Botany*, 101(1), 165–173.

Han, J., Lei, Z., Flexas, J., Zhang, Y., Carriquí, M., Zhang, W. et al. (2018) Mesophyll conductance in cotton bracts: anatomically determined internal CO_2 diffusion constraints on photosynthesis. *Journal of Experimental Botany*, 69(22), 5433–5443.

Hanson, D.T., Renzaglia, K. & Villarreal, J.C. (2014) Diffusion limitation and CO_2 concentrating mechanisms in bryophytes. In: Hanson, D. & Rice, S. (Eds.) *Photosynthesis in bryophytes and early land plants. Advances in photosynthesis and respiration (vol 37)*. Dordrecht, The Netherlands: Springer, pp. 95–111.

Hoppert, M., Reimer, R., Kemmling, A., Schröder, A., Günzl, B. & Heinken, T. (2004) Structure and reactivity of a biological soil crust from a xeric sandy soil in Central Europe. *Geomicrobiology Journal*, 21(3), 183–191.

Koster, K.L., Balsamo, R.A., Espinoza, C. & Oliver, M.J. (2010) Desiccation sensitivity and tolerance in the moss *Physcomitrella patens*: assessing limits and damage. *Plant Growth Regulation*, 62(3), 293–302.

Krall, J.P. & Edwards, G.E. (1992) Relationship between photosystem II activity and CO_2 fixation in leaves. *Physiologia Plantarum*, 86(1), 180–187.

Li, Y., Ren, B., Ding, L., Shen, Q., Peng, S. & Guo, S. (2013) Does chloroplast size influence photosynthetic nitrogen use efficiency? *PLoS One*, 8(4), e62036.

López-Pozo, M., Ballesteros, D., Laza, J.M., García-Plazaola, J.I. & Fernández-Marín, B. (2019) Desiccation tolerance in chlorophyllous fern spores: are ecophysiological features related to environmental conditions? *Frontiers in Plant Science*, 10, 1130.

López-Pozo, M., Flexas, J., Gulías, J., Carriquí, M., Nadal, M., Perera-Castro, A.V. et al. (2019) A field portable method for the semi-quantitative estimation of dehydration tolerance of photosynthetic tissues across distantly related land plants. *Physiologia Plantarum*, 167(4), 540–555.

Lu, Z., Lu, J., Pan, Y., Lu, P., Li, X., Cong, R. et al. (2016) Anatomical variation of mesophyll conductance under potassium deficiency has a vital role in determining leaf photosynthesis. *Plant, Cell & Environment*, 39(11), 2428–2439.

Moore, J.P., Farrant, J.M. & Driouich, A. (2008) A role for pectin-associated arabinans in maintaining the flexibility of the plant cell wall during water deficit stress. *Plant Signaling & Behavior*, 3(2), 102–104.

Moore, J.P., Vicré-Gibouin, M., Farrant, J.M. & Driouich, A. (2008) Adaptations of higher plant cell walls to water loss: drought vs desiccation. *Physiologia Plantarum*, 134(2), 237–245.

Morison, M.O. & Sheath, R.G. (1985) Responses to desiccation stress by *Klebsormidium rivulare* (Ulotrichales, Chlorophyta) from a Rhode Island stream. *Phycologia*, 24(2), 129–145.

Nadal, M., Brodribb, T.J., Fernández-Marín, B., García-Plazaola, J.I., Arzac, M.I., López-Pozo, M. et al. (2021) Differences in biochemical, gas exchange and hydraulic response to water stress in desiccation tolerant and sensitive fronds of the fern *Anemia caffrorum*. *New Phytologist*, 231(4), 1415–1430.

Nadal, M., Flexas, J. & Gulias, J. (2018) Possible link between photosynthesis and leaf modulus of elasticity among vascular plants: a new player in leaf traits relationships? *Ecology Letters*, 21(9), 1372–1379.

Nadal, M., Perera-Castro, A.V., Gulías, J., Farrant, J.M. & Flexas, J. (2021) Resurrection plants optimize photosynthesis despite very thick cell walls by means of chloroplast distribution. *Journal of Experimental Botany*, 72(7), 2600–2610.

Niinemets, Ü. & Reichstein, M. (2003a) Controls on the emission of plant volatiles through stomata: a sensitivity analysis. *Journal of Geophysical Research-Atmospheres*, 108(D7), 4211.

Niinemets, Ü. & Reichstein, M. (2003b) Controls on the emission of plant volatiles through stomata: differential sensitivity of emission rates to stomatal closure explained. *Journal of Geophysical Research*, 108(D7), 4208.

Nobel, P.S. (1991) *Physicochemical and environmental plant physiology*. San Diego: Academic Press.

Oliver, M.J., Cushman, J.C. & Koster, K.L. (2010) Dehydration tolerance in plants. In: Sunkar, R. (Ed.) *Plant stress tolerance*. Totowa: Humana Press, pp. 3–24.

Oliver, M.J., Farrant, J.M., Hilhorst, H.W., Mundree, S., Williams, B. & Bewley, J.D. (2020) Desiccation tolerance: avoiding cellular damage during drying and rehydration. *Annual Review of Plant Biology*, 71, 435–460.

Oliver, M.J., Velten, J. & Mishler, B.D. (2005) Desiccation tolerance in bryophytes: a reflection of the primitive strategy for plant survival in dehydrating habitats? *Integrative and Comparative Biology*, 45(5), 788–799.

Peguero-Pina, J.J., Sancho-Knapik, D. & Gil-Pelegrín, E. (2017) Ancient cell structural traits and photosynthesis in today's environment. *Journal of Experimental Botany*, 68(7), 1389–1392.

Pence, V.C., Dunford, S.S. & Redella, S. (2005) Differential effects of abscisic acid on desiccation tolerance and carbohydrates in three species of liverworts. *Journal of Plant Physiology*, 162(12), 1331–1337.

Perera-Castro, A.V., Flexas, J., González-Rodríguez, Á.M. & Fernández-Marín, B. (2021) Photosynthesis on the edge: photoinhibition, desiccation and freezing tolerance of Antarctic bryophytes. *Photosynthesis Research*, 149(1), 135–153.

Perera-Castro, A.V., Nadal, M. & Flexas, J. (2020) What drives photosynthesis during desiccation? Mosses and other outliers from the photosynthesis–elasticity trade-off. *Journal of Experimental Botany*, 71(20), 6460–6470.

Perera-Castro, A.V., Waterman, M.J., Turnbull, J.D., Ashcroft, M.B., McKinley, E., Watling, J.R. et al. (2020) It is hot in the sun: Antarctic mosses have high temperature optima for photosynthesis despite cold climate. *Frontiers in Plant Science*, 11, 1178.

Popper, Z.A. (2008) Evolution and diversity of green plant cell walls. *Current Opinion in Plant Biology*, 11(3), 286–292.

Popper, Z.A. & Fry, S.C. (2003) Primary cell wall composition of bryophytes and charophytes. *Annals of Botany*, 91(1), 1–12.

Popper, Z.A., Michel, G., Hervé, C., Domozych, D.S., Willats, W.G., Tuohy, M.G. et al. (2011) Evolution and diversity of plant cell walls: from algae to flowering plants. *Annual Review of Plant Biology*, 62, 567–590.

Pressel, S., Duckett, J.G., Ligrone, R. & Proctor, M.C. (2009) Effects of de- and rehydration in desiccation-tolerant liverworts: a cytological and physiological study. *International Journal of Plant Sciences*, 170(2), 182–199.

Pressel, S., P'ng, K.M. & Duckett, J.G. (2010) A cryo-scanning electron microscope study of the water relations of the remarkable cell wall in the moss *Rhacocarpus purpurascens* (Rhacocarpaceae, Bryophyta). *Nova Hedwigia*, 91, 289–299.

Proctor, M. (2001) Patterns of desiccation tolerance and recovery in bryophytes. *Plant Growth Regulation*, 35(2), 147–156.

Proctor, M.C., Nagy, Z., Csintalan, Z. & Takacs, Z. (1998) Water-content components in bryophytes: analysis of pressure-volume relationships. *Journal of Experimental Botany*, 49(328), 1845–1854.

Proctor, M.C., Oliver, M.J., Wood, A.J., Alpert, P., Stark, L.R., Cleavitt, N.L. et al. (2007) Desiccation-tolerance in bryophytes: a review. *The Bryologist*, 110(4), 595–621.

Proctor, M.C.F. (1999) Water-relations parameters of some bryophytes evaluated by thermocouple psychrometry. *Journal of Bryology*, 21(4), 263–270.

R Core Team. (2016) *R: a language and environment for statistical computing*. Vienna, Austria: R Foundation for Statistical Computing.

Ren, T., Weraduwage, S.M. & Sharkey, T.D. (2019) Prospects for enhancing leaf photosynthetic capacity by manipulating mesophyll cell morphology. *Journal of Experimental Botany*, 70(4), 1153–1165.

Reynolds, E.S. (1963) The use of lead citrate at high pH as an electron-opaque stain in electron microscopy. *Journal of Cell Biology*, 17(1), 208–212.

Rondeau-Mouro, C., Defer, D., Leboeuf, E. & Lahaye, M. (2008) Assessment of cell wall porosity in *Arabidopsis thaliana* by NMR spectroscopy. *International Journal of Biological Macromolecules*, 42(2), 83–92.

Sack, L. & Pasquet-Kok, J. (2011) Leaf pressure-volume curve parameters. PrometheusWiki. Available at: http://prometheuswiki.org/tiki-index.php?page=Leaf+pressure-volume+curve+parameters [Accessed 12th May 2021]

Salleo, S. & Gullo, M.L. (1990) Sclerophylly and plant water relations in three Mediterranean *Quercus* species. *Annals of Botany*, 65(3), 259–270.

Scheffer, R.A., Van Logtestijn, R.P. & Verhoeven, J.T.A. (2001) Decomposition of *Carex* and *Sphagnum* litter in two mesotrophic fens differing in dominant plant species. *Oikos*, 92(1), 44–54.

Sharkey, T.D. (2016) What gas exchange data can tell us about photosynthesis. *Plant, Cell & Environment*, 39(6), 1161–1163.

Sharkey, T.D., Bernacchi, C.J., Farquhar, G.D. & Singsaas, E.L. (2007) Fitting photosynthetic carbon dioxide response curves for C_3 leaves. *Plant, Cell & Environment*, 30(9), 1035–1040.

Shivaraj, Y.N., Barbara, P., Gugi, B., Vicré-Gibouin, M., Driouich, A., Govind, S.R. et al. (2018) Perspectives on structural, physiological, cellular, and molecular responses to desiccation in resurrection plants. *Scientifica*, 2018, 1–18. https://doi.org/10.1155/2018/9464592

Shrestha, B.B., Uprety, Y., Nepal, K., Tripathi, S. & Jha, P.K. (2007) Phenology and water relations of eight woody species in the coronation garden of Kirtipur, Central Nepal. *Himalayan Journal of Sciences*, 4(6), 49–56.

Smith, E.C. & Griffiths, H. (1996) A pyrenoid-based carbon-concentrating mechanism is present in terrestrial bryophytes of the class Anthocerotae. *Planta*, 200(2), 203–212.

Terashima, I., Hanba, Y.T., Tazoe, Y., Vyas, P. & Yano, S. (2006) Irradiance and phenotype: comparative eco-development of sun and shade leaves in relation to photosynthetic CO_2 diffusion. *Journal of Experimental Botany*, 57(2), 343–354.

Thain, J.F. (1983) Curvature correlation factors in the measurements of cell surface areas in plant tissues. *Journal of Experimental Botany*, 34(1), 87–94.

Théroux-Rancourt, G., Jenkins, M.R., Brodersen, C.R., McElrone, A., Forrestel, E.J. & Earles, J.M. (2020) Digitally deconstructing leaves in 3D using X-ray microcomputed tomography and machine learning. *Applications in Plant Sciences*, 8(7), e11380.

Tomás, M., Flexas, J., Copolovici, L., Galmés, J., Hallik, L., Medrano, H. et al. (2013) Importance of leaf anatomy in determining mesophyll diffusion conductance to CO_2 across species: quantitative limitations and scaling up by models. *Journal of Experimental Botany*, 64(8), 2269–2281.

Tomás, M., Medrano, H., Brugnoli, E., Escalona, J.M., Martorell, S., Pou, A. et al. (2014) Variability of mesophyll conductance in grapevine cultivars under water stress conditions in relation to leaf anatomy and water use efficiency. *Australian Journal of Grape and Wine Research*, 20(2), 272–280.

Tosens, T. & Laanisto, L. (2018) Mesophyll conductance and accurate photosynthetic carbon gain calculations. *Journal of Experimental Botany*, 69, 5315–5318.

Tosens, T., Niinemets, U., Vislap, V., Eichelmann, H. & Castro Diez, P. (2012) Developmental changes in mesophyll diffusion conductance and photosynthetic capacity under different light and water availabilities in *Populus tremula*: how structure constrains function. *Plant, Cell & Environment*, 35(5), 839–856.

Tosens, T., Niinemets, Ü., Westoby, M. & Wright, I.J. (2012) Anatomical basis of variation in mesophyll resistance in eastern Australian sclerophylls: news of a long and winding path. *Journal of Experimental Botany*, 63(14), 5105–5119.

Tosens, T., Nishida, K., Gago, J., Coopman, R.E., Cabrera, H.M., Carriquí, M. et al. (2016) The photosynthetic capacity in 35 ferns and fern allies: mesophyll CO_2 diffusion as a key trait. *New Phytologist*, 209(4), 1576–1590.

Turetsky, M.R. (2003) The role of bryophytes in carbon and nitrogen cycling. *Bryologist*, 106(3), 395–409.

Valentini, R., Epron, D., De Angelis, P., Matteucci, G. & Dreyer, E. (1995) *In situ* estimation of net CO_2 assimilation, photosynthetic electron flow and photorespiration in Turkey oak (*Q. cerris* L.) leaves: diurnal cycles under different levels of water supply. *Plant, Cell & Environment*, 18(6), 631–640.

Van Caemmerer, S. & Evans, J.R. (1991) Determination of the average partial pressure of CO_2 in chloroplasts from leaves of several C_3 plants. *Functional Plant Biology*, 18(3), 287–305.

Veromann-Jürgenson, L.L., Brodribb, T.J., Niinemets, Ü. & Tosens, T. (2020) Pivotal role of mesophyll conductance in shaping photosynthetic performance across 67 structurally diverse gymnosperm species. *International Journal of Plant Sciences*, 181(1), 116–128.

Wang, Z., Bader, M.Y., Pi, C., He, Y., Guo, S. & Bao, W. (2021) Does the removal of non-photosynthetic sections lead to a down-regulation of photosynthesis in mosses? A first experiment. *Cryptogamie, Bryologie*, 42(7), 117–127.

Wang, Z., Liu, X. & Bao, W. (2016) Higher photosynthetic capacity and different functional trait scaling relationships in erect bryophytes compared with prostrate species. *Oecologia*, 180(2), 359–369.

Watkins, J.J.E., Mack, M.C., Sinclair, T.R. & Mulkey, S.S. (2007) Ecological and evolutionary consequences of desiccation tolerance in tropical fern gametophytes. *New Phytologist*, 176(3), 708–717.

Webb, M.A. & Arnott, H.J. (1982) Cell wall conformation in dry seeds in relation to the preservation of structural integrity during desiccation. *American Journal of Botany*, 69(10), 1657–1668.

Wei, T., Simko, V., Levy, M., Xie, Y., Jin, Y. & Zemla, J. (2017) Package "corrplot". *Stat*, 56, e24.

Wickham, H. (2007) Reshaping data with the reshape package. *Journal of Statistical Software*, 21, 1–20.

Wickham, H. (2011) The Split-apply-combine strategy for data analysis. *Journal of Statistical Software*, 40, 1–29.

Wickham, H. (2016) *ggplot2: elegant graphics for data analysis*. New York: Springer-Verlag.

Wood, A.J. (2007) The nature and distribution of vegetative desiccation-tolerance in hornworts, liverworts and mosses. *The Bryologist*, 110(2), 163–177.

Yin, X., Sun, Z., Struik, P.C. & Gu, J. (2011) Evaluating a new method to estimate the rate of leaf respiration in the light by analysis of combined gas exchange and chlorophyll fluorescence measurements. *Journal of Experimental Botany*, 62(10), 3489–3499.

Zhang, W.H. (1998) Water relations balance parameters of 30 woody species from Cerrado vegetation in the wet and dry season. *Journal of Forestry Research*, 9(4), 233–239.

SUPPORTING INFORMATION

Additional supporting information may be found in the online version of the article at the publisher's website.

How to cite this article: Perera-Castro, A.V. & Flexas, J. (2022) Desiccation tolerance in bryophytes relates to elasticity but is independent of cell wall thickness and photosynthesis. *Physiologia Plantarum*, 174(2), e13661. Available from: https://doi.org/10.1111/ppl.13661